ANALYTICAL SCIENCES JUNE 2019, VOL. 35

Original Papers

Amplification of Sensor Signals from Metal Mesh Device with Fine Periodic Structure

Hirokazu SETO,*1† Atsushi SAIKI,*1 Seiji KAMBA,*2 Takashi KONDO,*2 Makoto HASEGAWA,*3 Yoshiko MIURA,*4 Yumiko HIROHASHI,*1 and Hiroyuki SHINTO*1

*1 *Department of Chemical Engineering, Fukuoka University, 8-19-1 Nanakuma, Jonan, Fukuoka 814–0180, Japan*
*2 *Murata Manufacturing Co., 1-10-1 Higashikotari, Nagaokakyo, Kyoto 617–8555, Japan*
*3 *Graduate School of Bioscience, Nagahama Institute of Bio-Science and Technology, 1266 Tamura, Nagahama, Shiga 526–0829, Japan*
*4 *Graduate School of Engineering, Kyushu University, 744 Motooka, Nishi, Fukuoka 819–0395, Japan*

Two types of metal mesh devices with hole diameters of 1.7 and 0.3 μm were prepared by an electroforming method. The metal mesh devices with hole diameters of 1.7 and 0.3 μm transmitted electromagnetic waves with frequencies of approximately 100 and 285 THz, respectively. These spectral frequencies shifted depending on the adsorption amount of protein. The slope in the linear relationship between the adsorption amount and spectral shift (*i.e.* sensitivity) of the metal mesh device with a hole diameter of 0.3 μm was seven times as great as that of the device with a hole diameter of 1.7 μm. These results agreed with the theoretical concept of the sensitivity for the metal mesh device sensor being proportional to the square of the transmittance frequency. As biosensors, the structurally refined metal mesh devices amplified the output signals.

Keywords Metal mesh device, biosensor, biotin-avidin interaction, sensitivity amplification, structural refinement

(Received November 14, 2018; Accepted January 24, 2019; Advance Publication Released Online by J-STAGE February 1, 2019)

Introduction

A biosensor consists of a molecular recognition interface, which binds to a particular target, and a transducer, which converts a biochemical reaction to an output signal. As examples of the transducer, electrochemical and field-effect transistor sensors convert reactions to voltage-current changes.[1,2] Microcalorimetric sensors detect the heat produced by chemical reactions.[3] Surface plasmon resonance (SPR) sensors detect the refractive index change.[4,5] In quartz crystal microbalance (QCM) and surface acoustic wave sensors, the oscillation frequency is the output signal.[6,7] There exist two approaches toward the intensification of biosensor sensitivity: one is the advanced design of molecular recognition interfaces, wherein, the ability of the interface to bind with the target is improved by controlling the ligand density and orientation. Another is the improvement of the transducer, wherein, the output signals converted by the transducer are amplified by some means.

Metal mesh devices (MMDs) with numerous well-regulated holes have unique spectroscopic properties such as the selectivity of transmittance frequency.[8] The transmittance frequency depends on the periodic structure of the surface.[9] When a substance attaches to the surface of an MMD, the effective dielectric constant of the MMD changes from the dielectric constant of air to that of the substance. In an equivalent circuit model, the resonant frequency decreases as the dielectric constant increases. Consequently, the transmittance spectrum shifts to lower frequencies. MMD sensors have been developed utilizing this phenomenon, and applied to determine the concentration or quantity of a substance from the spectral shift.[10-23] The biggest advantage of the MMD sensor is the diversity of the target size, *i.e.*, MMD sensing can cover targets with a wide range of sizes (from microsize to nanosize), owing to the selection of an appropriate MMD hole size. In a previous study, we applied the MMDs with different hole sizes to the collection and detection of particulate matter with different particle sizes in air.[17] In the biosensing field, MMDs with a hole diameter of 1.8 μm that transmit electromagnetic waves with a frequency of approximately 100 THz selectively and quantitatively detect proteins and bacteria utilizing bioaffinity such as biotin-streptavidin, saccharide-lectin, and antigen-antibody interactions.[15,18,19] Hasegawa and coworkers were successful in detecting mammalian cells using an MMD.[20] When proteins were targeted, the detection limits of the MMD sensor, which was operated at 100 THz, were close to those of the QCM and SPR. Sensitivity can be further enhanced by improving the MMD as transducer.

In a previous study, we demonstrated computationally and experimentally that the sensitivity of the MMD sensor is proportional to the square of the transmittance frequency.[21] Moreover, the transmittance frequency is inversely proportional to the periodic size of the MMD. The MMDs used in previous

† To whom correspondence should be addressed.
E-mail: hirokazuseto@fukuoka-u.ac.jp

biosensing studies had hole diameters of larger than 1 μm, and operated in the middle-infrared (IR) frequency range. Higher detectability is expected by the structural refinement of the MMD, *i.e.*, fabricating the MMD with smaller holes, because refined MMDs operate in a higher frequency range (*i.e.*, near-IR region).

In this study, we developed MMDs with a hole size that was less than half the hole size of previously developed MMDs, based on research on MMD manufacturing techniques. The biosensor sensitivity (spectral shift per adsorption amount of protein) was amplified using MMDs with hole diameters of hundreds of nanometers. The biotin-avidin interaction was used as the model bioaffinity. After the MMDs were coated with gold, a self-assembled monolayer of thiol-terminated alkyl biotin was formed according to the hard and soft acids and bases theory.[24,25] The adsorption amounts of avidin onto the MMDs were determined, and the spectral shifts of the refined MMDs were compared with those of previously reported MMDs. The effect of structural refinement on sensor sensitivity was investigated.

Experimental

Reagents and materials

Thiol-terminated alkyl biotin (HS-$(CH_2)_{11}$-NH-C(O)-biotin) (ProChimia Co., Gdansk, Poland) was used for the formation of a biotinylated surface. Avidin (Wako Pure Chemical Industries Ltd., Osaka, Japan) was used as a protein probe. Poly(acrylamide) gel (e-PAGEL, cut off molecular weight: 14 – 250 kDa, ATTO Corporation, Tokyo, Japan) was used in electrophoresis experiments. Silver staining kit (Cosmo Bio, Tokyo, Japan) and SYPRO red (Molecular Probes, Eugene, OR, USA) were used as staining reagents in electrophoresis experiments. The eluent was prepared by adding DL-dithiothreitol (100 mmol L^{-1}), bromophenol blue (75 μmol L^{-1}), sodium dodecyl sulfate (69 mmol L^{-1}), and glycerol (10 wt%) to a Tris–HCl buffer solution (6 mmol L^{-1}, pH: 6.8), and was then used for the elution of avidin from the MMD.

Two types of MMDs with different hole diameters, which were made from nickel, were manufactured using the electroforming method. The thickness of the MMDs was approximately 1 μm. The hole size of the MMDs was controlled by a resist pattern used during the electroforming method. Then, the MMDs were coated with gold thin film (thickness of dozens of nanometers) by electroless deposition. Gold coating was performed to decrease the surface impedance and to form the self-assembled monolayer of the thiol-terminated alkyl biotin. The MMD surfaces were observed by scanning electron microscopy (SEM, VE-8800, Keyence Corporation, Osaka, Japan). The MMDs with hole diameters of 1.7 and 0.3 μm, respectively, were obtained.

Surface modification of MMDs

The MMDs were washed with acetone, ethanol, and water. After drying, both sides of the MMDs were ultraviolet-exposed (wavelength: 172 nm). The MMD surfaces were modified with biotin. The MMDs were immersed into a thiol-terminated alkyl biotin solution (ethanol:chloroform = 1:1) with a concentration of 500 mg L^{-1} for 20 h, washed with ethanol, and then dried. The biotinylation process was confirmed by X-ray photoelectron spectroscopy (XPS, Quantum2000, Physical Electronics, Inc., Chanhassen, MN, USA). The XPS spectra were calibrated using the peak corresponding to Au($4p^{7/2}$) at 84.0 eV.

Adsorption of avidin onto biotinylated MMD

The biotinylated MMD transmittance properties were evaluated prior to the protein adsorption process. The transmittance spectra of the MMDs with a hole diameter of 1.7 μm were recorded by an IR spectrometer (Spectrum 100 FTIR spectrometer, PerkinElmer Inc., Waltham, MA). The transmittance spectra of the MMDs with smaller holes were recorded by a near-IR spectrometer (NIRQuest512, Ocean Optics Inc., Dunedin, FL, USA) attached with a tungsten halogen light source (HL-2000, Ocean Optics Inc.) and integrating sphere (FOIS-1, Ocean Optics Inc.). The effective spot diameter of the MMDs was 6 mmϕ.

Avidin was detected using the biotinylated MMDs with different hole sizes. The biotinylated MMDs were immersed in a phosphate-buffered solution (10 mmol L^{-1}, pH: 7.4) of avidin at 40°C for 2 h. The MMDs were then washed with a sufficient quantity of water using a shaker for over 30 min, and then dried. The transmittance spectra of the biotinylated MMDs were determined after the protein adsorption process by the abovementioned method. The shift level in the spectrum (Δf) was estimated from the difference between the transmittance frequencies before and after the protein adsorption, and was corrected based on the shifts observed for the MMD incubated in buffer.

Electrophoresis experiments for avidin quantification

The adsorption amounts of avidin on the MMDs were determined by following the elution from the biotinylated MMDs. MMDs adsorbed with avidin were immersed in the eluent at 98°C for 5 min. The resulting solutions were spotted onto the poly(acrylamide) gel, which was then fractionated by electrophoresis for 1 h. The fractions of avidin on the gel were visualized using staining reagents. The concentration of avidin in the eluent was estimated from the total gray value of the electrophoretic band, which was obtained using the ImageJ software (National Institutes of Health, Bethesda, MD, USA). The adsorption amount of avidin onto the biotinylated MMDs (q, mol mm^{-2}) was calculated as follows:

$$q = C \times v/A$$

where C, v, and A are the concentration of avidin in the eluent, volume of eluent, and effective surface area of the metallic part of the MMD, respectively.

Results and Discussion

MMD properties

Two types of MMDs with different hole diameters (1.7 and 0.3 μm) were manufactured (Fig. 1). The hole shape of the MMD with a hole diameter of 0.3 μm became rounded, because the curvature of the corner increased by decreasing the hole size in the manufactured MMD. The variabilities in hole diameters were approximately 20 nm. The grid intervals of the MMDs with hole diameters of 1.7 and 0.3 μm were 2.5 and 1.0 μm, respectively. The hole numbers of the MMDs were estimated at 1.45×10^5 holes mm^{-2} (aperture ratio: 46%) and 1.06×10^6 holes mm^{-2} (aperture ratio: 7%), respectively. Both types of MMDs had a well-regulated periodic structure.

The transmittance spectra of the MMDs with hole diameters of 1.7 and 0.3 μm are shown in Fig. 2. The MMDs with hole diameters of 1.7 and 0.3 μm transmitted electromagnetic waves with frequencies of 99.2 ± 0.9 and 283.6 ± 0.6 THz, respectively. In previous studies, a dipped peak, which is the bottom point of

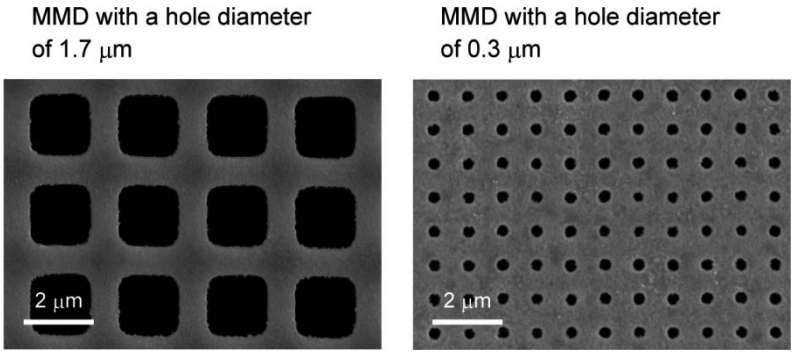

Fig. 1 SEM images of MMD surfaces with hole diameters of 1.7 and 0.3 μm before biotinylation.

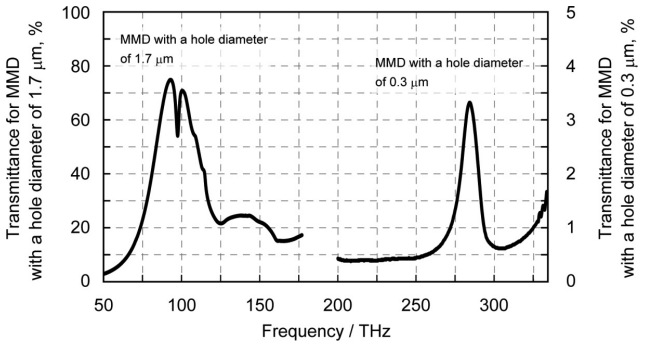

Fig. 2 Transmittance spectra of MMDs with different hole sizes before biotinylation.

the transmittance waveform in a passband, has been observed in spectra of MMDs with a hole diameter greater than 1 μm.[15,17–23] Our MMDs with hole diameters of 1.7 μm also had a dipped peak in their spectra. The Δf for the MMDs with a hole diameter of 1.7 μm is defined as the difference between the frequencies at the dipped peak before and after protein adsorption. However, a dipped peak did not appear in the spectrum of the MMD with smaller holes. Consequently, the Δf for the MMDs with a hole diameter of 0.3 μm is defined as the difference between the transmittance frequencies at the peak top in a passband before and after protein adsorption. The electromagnetic-field simulations indicated that the disappearance of the dipped peak was caused by the round shape of the hole and particularly the decrease of the aperture ratio (Figs. S1 and S2, Supporting Information). The dipped peak of the MMD with a round shape was shallower than that of the MMD with a square hole, and gradually disappeared as the aperture ratio decreased.

The sensitivity of the MMD sensor is proportional to the square of the transmittance frequency (f_0), as follows,[21]

$$\text{Sensitivity} = a \times (f_0)^2$$

where the coefficient a is 4.45×10^6 mm^2 ng^{-1} THz^{-1} for protein detection. It is thought that MMDs with a hole diameter of 0.3 μm result in an 8.1-fold amplification of sensitivity, in comparison to the MMDs with a hole diameter of 1.7 μm. In simulations, the sensitivities of the MMDs with square and round holes at the same aperture ratio were approximately the same (Figs. S3 and S4, Supporting Information). Therefore, the effect of the hole shape on the sensitivity was negligible.

Biotinylation of MMDs

The XPS of the unmodified and biotinylated MMDs was measured (Fig. 3). Similar to the MMDs with hole diameters of 1.7 and 0.3 μm, the peaks relating to nitrogen and sulfur atoms in the biotin reagent appeared at 400 and 164 eV, respectively, in the spectra after biotinylation. The double peaks at 84 and 88 eV were attributed to the $4f^{7/2}$ and $4f^{5/2}$ orbitals of gold, and these intensities decreased by half after the biotinylation of the MMDs. The results confirmed that the biotin layer was successfully formed on the MMDs. Additionally, they were not so different in comparison to the elemental ratios of nitrogen atoms (or sulfur atoms) to gold atoms on the biotinylated MMDs with hole diameters of 1.7 and 0.3 μm (Table 1). It is suggested that the biotin densities on the surface of the MMDs with hole diameters of 1.7 and 0.3 μm were similar.

Detection of protein using biotinylated MMDs

The biotinylated MMDs with hole diameters of 1.7 and 0.3 μm were adsorbed with avidin, and their transmittance spectra were measured (Fig. S5, Supporting Information). The transmittance spectra of both MMDs were shifted toward lower frequencies. The Δf values of the biotinylated MMDs with hole diameters of 1.7 and 0.3 μm after the adsorption of avidin at different concentrations are shown in Fig. 4. The Δf values of the biotinylated MMDs increased with increasing avidin concentration, and eventually reached respective saturation values. The apparent binding constant between the biotin and avidin (K_a) and the maximum shift level in the spectrum (Δf_{max}) were estimated by the Langmuir equation, assuming monolayer adsorption of avidin. The K_a values of the biotinylated MMDs with hole diameters of 1.7 and 0.3 μm were 0.95×10^7 and 1.16×10^7 L mol^{-1}, respectively. The binding abilities of the biotin on the MMDs with different hole diameters were not so different, whereas, the Δf_{max} values were quite different. Specifically, the Δf_{max} values of the biotinylated MMDs with hole diameters of 1.7 and 0.3 μm were 0.27 and 2.11 THz, respectively. The limits of detection for the biotinylated MMDs with hole diameters of 1.7 and 0.3 μm, as calculated by $3.29 \times \sigma_0$, were similar at 4.91×10^{-8} and 1.55×10^{-8} mol L^{-1}, respectively.

The q value was determined after the elution of avidin from the biotinylated MMDs. The Δf for the biotinylated MMDs with hole diameters of 1.7 and 0.3 μm as a function of q is shown in Fig. 5. The correlation between the values of Δf and q was relatively linear. The slopes (corresponding to sensitivity) of the biotinylated MMDs with transmittance frequencies of 99.2 and 283.6 THz agreed with the slopes obtained by the previously reported simulation.[21] The slope for the biotinylated

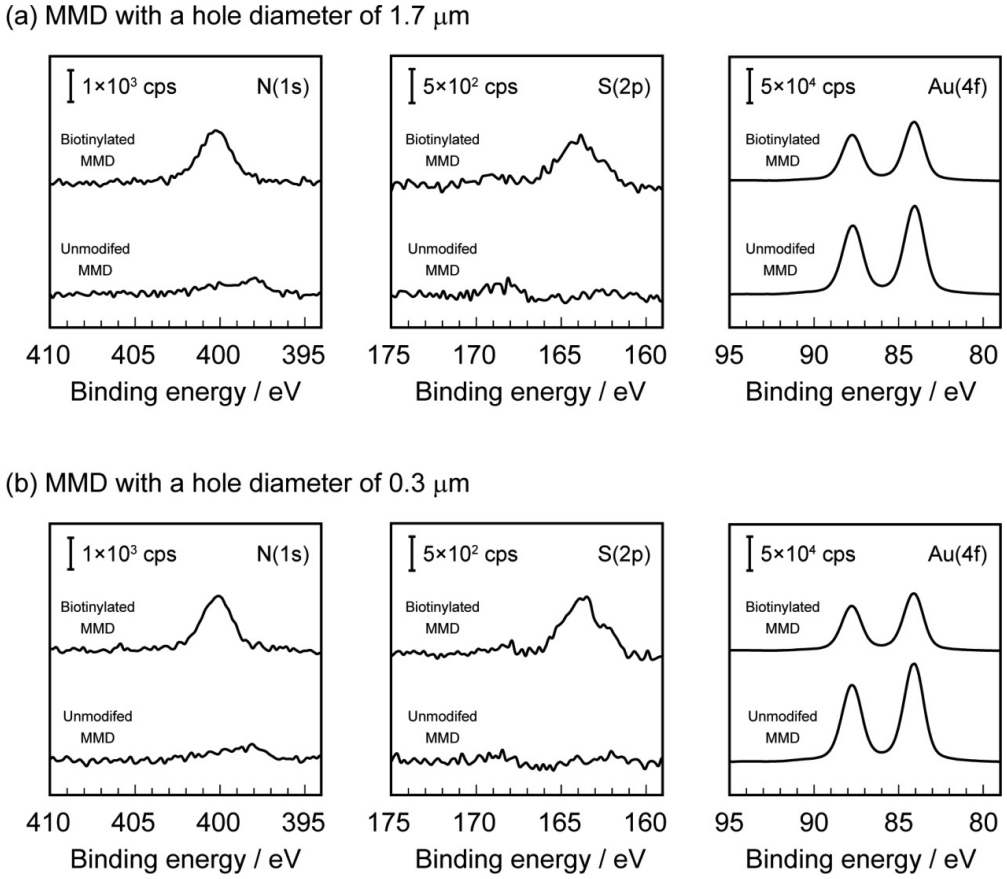

Fig. 3 XPS spectra of MMDs with different hole sizes before and after biotinylation.

Table 1 Elemental ratios of nitrogen and sulfur atoms to gold atoms on MMDs with different hole sizes

	Unmodified MMD with a hole diameter of 1.7 μm	Biotinylated MMD with a hole diameter of 1.7 μm	Unmodified MMD with a hole diameter of 0.3 μm	Biotinylated MMD with a hole diameter of 0.3 μm
N/Au	0.070 ± 0.004	0.297 ± 0.012	0.080 ± 0.018	0.270 ± 0.027
S/Au	0.023 ± 0.002	0.077 ± 0.003	0.019 ± 0.001	0.069 ± 0.013

MMDs with a hole diameter of 0.3 μm was seven times larger than that with a hole diameter of 1.7 μm. This result was close to the theoretical value, because the sensitivity of the MMD sensor is proportional to the square of the transmittance frequency. The sensing mechanism of the MMDs was attributed to the localization of an electromagnetic field on their surfaces. The incursion of an analyte into the localized electromagnetic field leads to the shift of the transmittance spectrum, owing to the change in the complex refractive index of the nearby surface. The thickness of the localized electromagnetic field shrinks as the transmittance frequency of the MMD increases.[16] When MMDs with high transmittance frequency are used, the ratio of the localized electric field occupied by a small analyte, such as protein, is enhanced. Consequently, as biosensors, the structurally refined MMDs amplified the output signals.

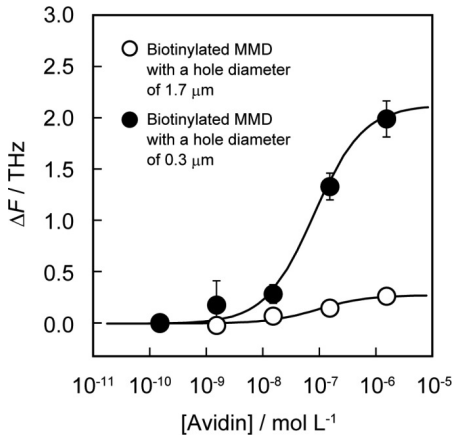

Fig. 4 Shift levels in spectra of biotinylated MMDs with different hole sizes after adsorption of avidin at different bulk concentrations. Error bars were determined from five different samples. Standard deviations of the blank samples (σ_0) for the biotinylated MMDs with hole diameters of 1.7 and 0.3 μm were 0.026 and 0.097 THz, respectively. Solid lines represent curve fit based on the Langmuir equation. $R^2 = 0.959$ (biotinylated MMD with hole diameter of 1.7 μm) and $R^2 = 0.993$ (biotinylated MMD with hole diameter of 0.3 μm).

Conclusions

This study investigated the effect of structural refinement on the sensitivity of an MMD sensor. When the hole size of the MMDs

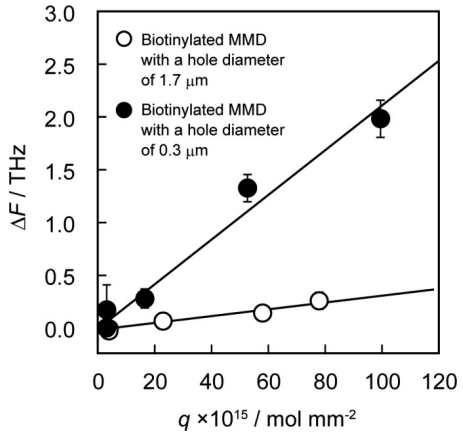

Fig. 5 Relationship between the shift levels in spectra of biotinylated MMDs with different hole sizes after adsorption of avidin and the adsorption amounts of avidin onto biotinylated MMDs. Error bars were determined from more than two different samples. Slopes of the biotinylated MMDs with hole diameters of 1.7 and 0.3 μm were 3.01×10^{12} and 2.10×10^{13} THz mm^2 mol^{-1}, respectively.

was reduced from several micrometers to hundreds of nanometers, a seven-fold increase in sensitivity was observed. As biosensors, the structurally refined MMDs enabled the amplification of the output signals. We are preparing MMDs with smaller holes than the current study. When the periodic structure of the MMD is more scaled down, the operating frequency finally enters the visible light region (400 – 750 THz). Because the thickness of the localized electric field on the MMD, which operates in this region, is in the same order as the protein size, a further enhancement of sensitivity is expected. In biosensing, small noises as well as large signals are also important. In future work, a high-performance biosensor should be developed by designing, fabricating, and evaluating the periodic MMD structure in order to prevent noise.

Acknowledgements

This work was supported by funds from the Hosokawa Powder Technology Foundation, Kurita Water and Environment Foundation, Shiraishi Scientific Research Fund of Fukuoka University, and Central Research Institute of Fukuoka University (No. 175009). This work was funded by JSPS KAKENHI Grant No. 16H04557.

Supporting Information

Results of electromagnetic-field simulations for the MMDs are provided in Supporting Information. This material is available free of charge on the Web at http://www.jsac.or.jp/analsci/.

References

1. N. J. Ronkainen, H. B. Halsall, and W. R. Heineman, *Chem. Soc. Rev.*, **2010**, *39*, 1747.
2. L. Torsi, M. Magliulo, K. Manoli, and G. Palazzo, *Chem. Soc. Rev.*, **2013**, *42*, 8612.
3. I. Wadsö, *Chem. Soc. Rev.*, **1997**, *26*, 79.
4. J. Homola, S. S. Yee, and G. Gauglitz, *Sens. Actuators, B*, **1999**, *54*, 3.
5. J. Homola, *Chem. Rev.*, **2008**, *108*, 462.
6. C. K. O'Sullivan and G. G. Guilbault, *Biosens. Bioelectron.*, **1999**, *14*, 663.
7. J. Devkota P. R. Ohodnicki, and D. W. Greve, *Sensors*, **2017**, *17*, 801.
8. R. Ulrich, *Infrared Phys.*, **1967**, *7*, 37.
9. S. Yoshida, K. Suizu, E. Kato, Y. Nakagomi, Y. Ogawa, and K. Kawase, *J. Mol. Spec.*, **2009**, *256*, 146.
10. F. Miyamaru, S. Hayashi, C. Otani, K. Kawase, Y. Ogawa, H. Yoshida, and E. Kato, *Opt. Lett.*, **2006**, *31*, 1118.
11. H. Yoshida, Y. Ogawa, Y. Kawai, S. Hayashi, A. Hayashi, C. Otani, E. Kato, F. Miyamaru, and K. Kawase, *Appl. Phys. Lett.*, **2007**, *91*, 253901.
12. Y. Ogawa, S. Hayashi, C. Otani, and K. Kawase, *PIERS Online*, **2008**, *4*, 396.
13. S. Yoshida, E. Kato, K. Suizu, Y. Nakagomi, Y. Ogawa, and K. Kawase, *Appl. Phys. Express*, **2009**, *2*, 012301.
14. T. Kondo, S. Kamba, K. Takigawa, T. Suzuki, Y. Ogawa, and N. Kondo, *Procedia Eng.*, **2011**, *25*, 916.
15. H. Seto, C. Yamashita, S. Kamba, T. Kondo, M. Hasegawa, M. Matsuno, Y. Ogawa, and Y. Miura, *Langmuir*, **2013**, *29*, 9457.
16. T. Suzuki, T. Kondo, Y. Ogawa, S. Kamba, and N. Kondo, *IEEE Sens. J.*, **2013**, *13*, 4972.
17. H. Seto, S. Kamba, T. Kondo, Y. Ogawa, Y. Hoshino, and Y. Miura, *Chem. Lett.*, **2014**, *43*, 408.
18. H. Seto, S. Kamba, T. Kondo, M. Hasegawa, S. Nashima, Y. Ehara, Y. Ogawa, Y. Hoshino, and Y. Miura, *ACS Appl. Mater. Interfaces*, **2014**, *6*, 13234.
19. H. Seto, S. Kamba, T. Kondo, Y. Ogawa, Y. Hoshino, and Y. Miura, *Anal. Sci.*, **2015**, *3*, 173.
20. M. Hasegawa, K. Yamamoto, E. Shirai-Kitanishi, K. Mori, Y. Inoue, Y. Inagaki, R. Sasaki, T. Mizukami, N. Shirai, Y. Miura, Y. Ogawa, M. Banju, S. Kamba, and T. Kondo, *IEEE Sens. J.*, **2016**, *16*, 5129.
21. S. Kamba, H. Seto, T. Kondo, and Y. Miura, *Anal. Sci.*, **2017**, *33*, 1033.
22. S. Kamba, H. Seto, T. Kondo, and Y. Miura, *Anal. Sci.*, **2018**, *34*, 547.
23. S. Kamba, H. Seto, T. Kondo, and Y. Miura, *Anal. Sci.*, **2018**, *34*, 765.
24. R. G. Peaeson, *J. Am. Chem. Soc.*, **1963**, *85*, 3533.
25. R. G. Peaeson, *Science*, **1966**, *151*, 172.